Virtual Generator-Storage Pairing for Robust Multistage Decisions in Power Systems

Yihan Zou, *Student Member, IEEE,* Xiaojun Lin, *Fellow, IEEE,* Dionysios Aliprantis, *Senior Member, IEEE,* Minghua Chen, *Fellow, IEEE*

***Abstract*—In this work, we present a robust optimization based framework for day-ahead reliability assessment (RA) and real-time dispatch to ensure power system reliability under multi-stage renewable uncertainty. Our framework jointly considers fossil-fuel generators and energy storage in the system. To obtain near-optimal performance in grid reliability, we develop robust multi-stage decisions based on the concept of "safe-dispatch sets" in the literature. Although such safe-dispatch sets directly answer the RA and real-time dispatch problem, their computation often incurs high computational complexity. To develop low-complexity algorithms, we adopt a divide-and-conquer paradigm. First, we derive the conditions to describe the safe-dispatch sets for a pair of energy storage and generator. The results from this simple building block provide us with useful insights on how the grid reliability is related to the parameters, e.g, the generators' ramp speeds and the storage capacity. To tackle the general multi-bus scenario, the uncertainty is split among virtual generator-storage pairs (VGSPs), where we can utilize the results from the one-bus building block. Numerical studies on a standard IEEE 30-bus test case illustrate that our proposed solution requires much lower storage capacity to ensure system reliability compared to state-of-the-art approaches, without renewable curtailment.**

***Index Terms*—reliability assessment, energy storage, renewable uncertainty, multistage decisions, generator-storage pairs.**

I. Introduction

The reliability of power system is challenged by the high penetration of volatile renewable resources, e.g., solar and wind energy [1]. One of the most crucial grid operations that face new difficulty is to maintain the demand-supply balance at all time, under various physical constraints in the grid. In particular, under high renewable uncertainty, it becomes harder to determine the amount of resource commitment ahead of time, as well as the real-time dispatch of the committed resources. Meanwhile, energy storage has been considered as a key resource to improve the power system resilience because of its capability of shifting the demand and supply over periods [2]. However, energy storage has its unique characteristics compared to conventional fossil-fuel generators. Hence, to maintain system reliability, new questions need to be answered on how to jointly control conventional generators and energy storage in an optimal manner.

Manuscript received... Yihan Zou is with ByteDance Inc., Mountain View, CA 94041 (email: yihan.zou@bytedance.com). Xiaojun Lin and Dionysios Aliprantis are with Purdue University, West Lafayette, IN 47906 (email: linx@purdue.edu; dionysios@purdue.edu). Minghua Chen is with City University of Hong Kong, HKSAR, China (email: minghua.chen@cityu.edu.hk).

This work has been supported in part by NSF grants ECCS-1509536 and CCF-1442726, a Start-up Grant from School of Data Science, City University of Hong Kong (Project No. 9380118), and a General Research Fund from Research Grants Council, Hong Kong (Project No. 11206821).

In this work, we aim to address these problems at the Independent System Operator (ISO) level. The main responsibility of an ISO is to ensure grid reliability in a large geographic area, by managing the wholesale electricity market [3]–[5]. The wholesale market usually consists of the following two components. 1) A *day-ahead market* takes and clears bids from market participants for the buying/selling amount of energy one day before the operating day. 2) A *real-time market* occurs at the operation day, where the ISO can send real-time dispatch decisions to all committed resources in 5-min intervals in order to account for any demand deviation from the predicted amount. Further, after the day-ahead market clears (and thus unit commitment decisions have been made), the ISO performs a Reliability Assessment and Commitment (RAC) step to ensure the committed grid resources are adequate for the next operating day. The goal of this paper is to study reliability assessment (RA) during the RAC step[1], and to provably ensure grid reliability in real-time dispatch, for systems with conventional generators and energy storage under high renewable uncertainty.

For a more accurate model of this control and decision problem, one must consider the multistage nature of the renewable uncertainty. Here, the multiple stages refer to the moments when the uncertainty is revealed, i.e., the actual realization of the renewable generation is available sequentially over time. Yet, the ISO must make dispatch decisions using only the observations up to the current time, despite any future uncertainty. Any practical decision making process must respect such *causality* (or *non-anticipativity*) requirement. In contrast, a two-stage model has often been adopted in many related studies in the literature, which violates the above multistage nature. Specifically, a two-stage model assumes a second phase in the decision making process, where the entire uncertainty would be unveiled [6], [7]. Clearly, the assumption of the second phase with perfect knowledge is impractical. As a consequence, the resource requirement for reliability can be significantly under-estimated by any two-stage approach [8], [9]. In the literature, Model Predictive Control (MPC) is also studied for control under uncertainty [10]. Further, it is possible to iteratively apply a two-stage method in a rolling-horizon manner under multistage uncertainty [11]. However, since these approaches do not explicitly consider the multistage nature of future uncertainty, they typically do not provide the required reliability guarantees at the ISO level.

There have been limited studies in the literature that account

[1]Note that our study focuses on the first step of RAC (i.e., assessing reliability) and the associated real-time dispatch (if the system is reliable).

for such a multistage nature while ensuring grid reliability, especially for the systems with energy storage. In [8], the authors propose Affinely Adjustable Robust Optimization (AARO) policies [12], [13] to solve this multistage decision problem for systems with only generators. The authors later extend this approach in [9] to work with energy storage. However, [8] and [9] both suffer from a common weakness, i.e., the affine policy treats heterogeneous resources in the same manner, resulting in inefficient usage of resources (see Sec. II-D for more discussion). Partly because of this reason, renewable curtailment must be allowed in [9] so that they can always achieve demand-supply balance despite this inefficiency. Intuitively, generators and energy storage have very different capabilities: generators can sustain longer-term changes in demand, while storage units can provide flexibility to accommodate fast short-term changes. If one can leverage their complementary capabilities, the system will be able to support a higher level of uncertainty. Therefore, we are interested in the following open question: how should one jointly operate the storage and generators in a complementary and efficient way, such that the grid reliability can be achieved against multistage renewable uncertainty?

To answer this open question, a new robust optimization framework for developing reliability assessment and real-time dispatch decisions is proposed to jointly operate generators and energy storage. Without any renewable curtailment, our methods successfully exploit the complementary characteristics of energy storage and conventional generators to outperform the affine policies in [9] in terms of grid reliability under renewable uncertainty. In particular, we extend the notion of "safe-dispatch sets" from [14] to our problem with energy storage in Sec. II. Roughly speaking, the safe-dispatch set contains all dispatch decisions at the present time that guarantee the existence of reliable dispatch decisions any time in the future. In our previous work [14], we have shown that day-ahead RA is equivalent to the task of verifying if the safe-dispatch set is non-empty. Similarly, for real-time dispatch, any decision points from the safe-dispatch set can be chosen in every time slot (see Sec. II-C). Theoretically, the safe-dispatch set maximally exploits the complementary capabilities of the grid resources, without the restriction of affine decisions. However, solving safe-dispatch sets in the most general form using dynamic programming incurs exponential complexity [14]. As the first step towards developing computationally-efficient and near-optimal methods, in Sec. III we study a generator-storage pair. For this simpler building block, both necessary conditions and sufficient conditions are derived for characterizing the safe-dispatch set, which are tight under certain circumstances. In this way, our characterization fully exploits the complementary capabilities in such a single-generator single-storage building block. As the second step, Sec. IV studies a general multi-bus system with arbitrary numbers of generators and storage. In particular, we conceptually group the generators and storage into "virtual generator-storage pairs" (VGSPs), so that we can optimize affine demand splitting to VGSPs. As a result, such a divide-and-conquer framework leads to a low-complexity characterization of a suitable subset of the true safe-dispatch set. Finally, our simulation results in Sec. V demonstrate significant improvement in reliability and generation cost over state-of-the-art affine policies [9].

Although similar demand splitting and resource pairing ideas have been used in [14] to exploit the complementary capabilities of fast and slow generators, we note that the techniques and analysis in this work are very different from [14] due to the introduction of energy storage. First, even for the single-bus case, unlike generators (which are the sole focus in [14]), the energy storage cannot supply/consume power for a long operation period due to its *limited energy capacity*, rendering the analysis of [14] inapplicable. Second, in the general multi-bus case, energy storage also introduces new and unique challenges: (i) the *efficiency loss* in charging/discharging leads to possible discrepancies between the states of the virtual storage units (in a VGSP) and that of the physical storage unit; (ii) since storage is more scarce, the generator and storage forming a VGSP may have to reside on different buses, which produces new uncertainty for meeting transmission-line constraints. See Sec. IV how new methods are developed to address these challenges.

Our preliminary work [15] assumed perfect charging/discharging efficiency for the energy storage. This work significantly extends the results in [15] to a storage model with efficiency loss, by overcoming the above-mentioned new challenges. Further, we present an intuitive example in Sec. II-D to demonstrate the gain of our proposed control policy over affine policies. We also significantly enhanced the numerical results in Sec. V. Finally, we include key proofs which are essential to our main results but absent in [15].

II. System Model

We use $\mathcal{B} = \{1,\ldots,N_b\}$ and $\mathcal{L} = \{1,\ldots,N_l\}$ to denote the sets of N_b buses and N_l transmissions lines, respectively. A discrete-time model is adopted in this work (i.e., the system time is equally divided into T time slots), which is commonly used in the literature [9], [14]. Given the day-ahead ON/OFF decisions of the generators and the storage units (i.e., unit-commitment decisions), our objective is to verify if the grid reliability can be assured by the committed resources for the whole operation period, and to dispatch them in real-time with assured reliability. The detailed notations are as follows.

A. System Components

1) Renewable Uncertainty and Net Demand: In this work, we treat the renewable generation as negative load, i.e., the renewable supply is subtracted from the actual load at bus b to get the uncertain net-demand $D_b(t)$ at time t. For any period from t_1 to t_2, we denote the net-demand sequence at bus b as $D_b(t_1{:}t_2)$, and define $D(t_1{:}t_2) \triangleq \{D_b(t_1{:}t_2), \forall b \in \mathcal{B}\}$. Note that this formulation implies no renewable curtailment in the system. This assumption can be justified by the following facts. First, some renewable generation sources are installed "behind-the-meter," e.g., rooftop solar panels, and thus cannot be easily controlled by the ISO. Second, renewable energy is oftentimes considered a more desirable source of energy, since it is cheaper and cleaner compared to fossil-fuel generation. In practice, renewable energy is sometimes curtailed in order

to ensure grid safety, at the price of sacrificing efficiency and economy. Therefore, developing such curtailment-free robust algorithms to ensure grid reliability is still an important problem both in theory and practice.

Now, let us present the model for uncertainty in net-demand. The uncertainty set D contains all possible sequences $D(1{:}t)$ that should be considered for the grid reliability. In this paper, we focus on the following uncertainty set:

$$D_b^{\min}(t) \quad D_b(t) \quad D_b^{\max}(t); \text{ for all } t; \tag{1}$$

$$jD_b(t_1) \quad D_b(t_2)j \quad {}_bjt_1 \quad t_2j; \text{ for all } t_1; t_2; \tag{2}$$

where $D_b^{\min}(t)$ and $D_b^{\max}(t)$ correspond to the net-demand lower and upper bounds, respectively, on bus b at time t. We use ${}_b \quad 0$ to denote the maximum net-demand variation per time slot on bus b. We model the inter-temporal change of renewable uncertainty as a Lipschitz constraint in (2). In practice, the parameters of the uncertainty set are obtained from historical data and forecast [16]. Notice that, even though the uncertainty set D contains all possible sequences $D(1{:}T)$, only $D(1{:}t)$ (the realization of net-demand *up to* t) is observed by ISO. In contrast to a two-stage model where the ISO knows the exact $D(1{:}T)$ at the second stage [6] [7], the multistage uncertainty requires the future values of $D(t{+}1{:}T)$ to remain unknown. Nonetheless, the future uncertainty given the revealed history can be refined based on (2), which can be considered as the "near-term prediction." In particular, given $D(1{:}t)$, the set of remaining net-demand sequences $D(t_1; t_2); t_1; t_2 > t$, will be smaller than (1) and (2), i.e.,

$$D^t_{[t_1:t_2]} = \{D(t_1{:}t_2)j \text{ there exist } D^0(1{:}T) \; 2 \; D, \text{ such that } D^0(1{:}t) = D(1{:}t), \text{ and } D^0(t_1{:}t_2) = D(t_1{:}t_2)\} :$$

Additionally, if $t_1 = t_2$, the above notation reduces to $D^t_{t_1}$.

2) Fossil-fuel Generators: The set of conventional generators in the system is denoted as $G = f1; 2; :::; N_g g$. Then, the power level $P_g(t)$ of generator $g \; 2 \; G$ at time t must satisfy

$$P_g^{\min} \quad P_g(t) \quad P_g^{\max}; 8g \; 2 \; G; t = 1; 2; : : : ; T; \tag{3}$$

where $P_g^{\min}$ and $P_g^{\max}$ are generator g's minimum and maximum power, respectively. Since storage by itself cannot support a long period of demand-supply imbalance, we assume that $\sum_{g2G} P_g^{\max} \quad \sum_{b2B} D_b^{\max}(t)$ and $\sum_{g2G} P_g^{\min} \quad \sum_{b2B} D_b^{\min}(t)$ for all time t. In addition, the following ramping constraint need to be satisfied:

$$jP_g(t+1) \quad P_g(t)j \quad R_g; t = 1; 2; : : : ; T \quad 1; \tag{4}$$

where R_g is the ramp rate of generator g. Finally, let $G_b \quad G$ be the set of generators at bus $b \; 2 \; B$.

3) Storage units: We use $S = f1; 2; :::; N_s g$ to denote the set of storage units in the system, where each $s \; 2 \; S$ has a finite capacity $\overline{Q}_s$. Let $Q_s(t)$ be the charge level of storage s at the end of time-slot t, and $Q_s(0)$ be the initial storage level of unit s. Thus, the following storage capacity constraints must be satisfied at all time:

$$0 \quad Q_s(t) \quad \overline{Q}_s; 8s \; 2 \; S; t = 0; 1; :::; T: \tag{5}$$

A unique feature of energy storage compared to generators is that the coupling of its charging and discharging actions across time. Assuming unit-length slot, we can express the power level of storage s during time-slot t as follows: for $t = 1; 2; :::; T;$

$$ {}_s(t) = \begin{cases} Q_s(t \quad 1) \quad Q_s(t); & Q_s(t \quad 1) > Q_s(t); \\ \frac{1}{{}_s}[Q_s(t \quad 1) \quad Q_s(t)]; & Q_s(t \quad 1) \quad Q_s(t); \end{cases} \tag{6}$$

where ${}_s \; 2 \; (0; 1]$ is the round-trip efficiency of the storage. Note that positive (or negative) signs of (t) correspond to the storage delivering (or absorbing) energy. The units of Q and are MWh and MWh/slot, respectively. Similar to [9], for ease of exposition we have assumed in (6) that the storage can be discharged without efficiency loss. Note that this assumption incurs no loss of generality, because the case where the energy storage has both charging efficiency ${}_{\text{char}}$ and discharging efficiency ${}_{\text{disc}}$ can always be mapped to a storage unit of form (6) by taking $Q^0_s(t) = {}_{\text{disc}} Q_s(t)$ and ${}_s = {}_{\text{disc}} \quad {}_{\text{char}}$. Finally, we use $\overline{}_s$ to denote the power limit of storage s, i.e., $j \; (t)j \quad \overline{}_s$ for all time t, and S_b to denote the set of storage units on bus b.

B. Demand-supply Balance & Transmission Constraints

In this paper, a DC power flow model is adopted [17]. To ensure grid reliability, the total power generation from generators and storage must be equal to the total net-demand at all time, i.e.,

$$\sum_{g2G} P_g(t) + \sum_{s2S} {}_s(t) = \sum_{b2B} D_b(t); t = 1; 2; : : : ; T: \tag{7}$$

Furthermore, we have to respect all transmission-line limits. For DC model of the transmission system, we let $S = [S_{l;b}]$ to denote the shift factor matrix, where $S_{l;b}$ is the power-flow contribution from bus b on line l. Thus, the power flow on line l at time t cannot exceed a value TL_l, i.e.,

$$\sum_{b=1}^{N_b} S_{l;b} \quad D_b(t) \quad \sum_{g2G_b} P_g(t) \quad \sum_{s2S_b} (t) \quad \text{TL}_l; \quad 8t = 1; 2; : : : ; T; 8l \; 2 \; L: \tag{8}$$

C. Objectives of Online Multistage Decisions

Let $\mathbf{P}(t) = [P_g(t); g \; 2 \; G]$ and $\mathbf{Q}(t) = [Q_s(t); s \; 2 \; S]$. Note that $\mathbf{Q}(t \quad 1)$ corresponds to the storage levels both at the end of time-slot $t \quad 1$ and at the beginning of time-slot t. We first introduce the following definitions.

Definition 1 (Causality)**.** Given an uncertainty set D, a real-time dispatch algorithm (D) is *causal* if, for every time t, the algorithm only uses $D(1{:}t)$ in producing the dispatch decision $V^{(D)}(t) = \{P_g{}^{(D)}(t); Q_s{}^{(D)}(t) \; jg \; 2 \; G; s \; 2 \; S\}$.

Definition 2 (Robustness)**.** A causal real-time dispatch algorithm (D) is *robust* if and only if, for all net-demand sequences $D(1{:}t) \; 2 \; D$ and at all time t, the dispatch decision $V^{(D)}(t)$ satisfies all physical constraints (3)-(8). Further, (D) is *robust given* $D(1{:}t)$ and $V^{(D)}(t)$ if and only if, for any possible future net-demand sequence $D(t{+}1{:}T) \; 2 \; D^t_{[t+1:T]}$, the dispatch output $V^{(D)}(t_1)$ produced by (D) will satisfy all constraints (3)-(8), for all $t_1 > t$.

Our goals of this study are twofold: (i) At the RAC stage, given the uncertainty set $\mathcal{D}$, determine if a causal and robust real-time dispatch algorithm $\Phi(\mathcal{D})$ exists; (ii) At time t, find $\Phi(\mathcal{D})$ and compute the dispatch decisions for the generators and storage units based on $D(1{:}t)$, so that all physical constraints can be satisfied. Note that the above causality requirement is a crucial difference between our online multistage decisions and two-stage formulations. (Readers may refer to [14] and [8] for more discussion.) Next, we define the notion of safe-dispatch set, which extends the similar concept in [14].

Definition 3 (Safe-Dispatch Set)**.** Given the revealed demand $D(1{:}t)$, the safe-dispatch set $F(D(1{:}t), Q(t-1))$ is defined as

$$F(D(1{:}t), Q(t-1)) = \{(P(t), Q(t)) \text{ starting from } Q(t-1), \exists \text{ a causal algorithm } \Phi \text{ (which produces } P(t), Q(t)) \text{ that both can balance the demand } D(t) \text{ subject to (3), (5)-(8) at time } t, \text{ and is } \textit{robust given } D(1{:}t) \textit{ for the future}\} \quad (9)$$

Our preliminary work [14] shows that, both the RA (reliability assessment) decisions and real-time dispatch algorithms can be easily derived from the safe dispatch sets. Specifically, the RA decision simply verifies the non-emptiness of the safe dispatch set without any net-demand realization, i.e., $F(\cdot,\cdot)$. For real-time dispatch at time t, the causal algorithm can simply choose any $V(t) \in F(D(1{:}t), Q(t-1))$[2] that is also reachable from $P(t-1)$. It is guaranteed that such decisions satisfy all future physical constraints. Moreover, such an algorithm is "maximally-robust," i.e., if this algorithm cannot ensure grid reliability, no other algorithms can do under the same uncertainty set $\mathcal{D}$. As shown in [14], one can compute the true safe-dispatch sets via backward induction or dynamic programming (DP). However, it is impractical to apply such a DP solution directly to large-scale power system problems, as the computation complexity grows exponentially in the problem size (*curse of dimensionality*). Hence, we aim to develop lower-complexity approaches for deriving the safe-dispatch sets in this paper.

D. An Example for the Inefficiency of Affine Policies

To motivate our new conditions for the safe-dispatch set, we first illustrate the inefficiency of the affine policy used in [9]. With storage, [9] computes storage dispatch decisions according to affine mappings of net-demand values, i.e.,

$$P_s^{\text{affine}}(t) = w_s(t) + \sum_{b} W_{b,s}(t)\,[D_b(t) - D_b^{\text{main}}(t)], \quad (10)$$

where $D^{\text{main}}(t)$ is the pre-determined baseline for each time t, and $w_s(t)$, $W_{b,s}(t)$ are pre-computed coefficients, subject to the robust constraints (3)-(8) for all $D(1{:}T) \in \mathcal{D}$. Suppose that $D^{\max}(t) - D^{\min}(t) = 1$ for all t, and the rate of change is ± 1. Suppose that the generator's power range is large enough for the uncertainty set, but its ramp rate $R_g = 1/n$ is limited, where $n > 1$ is a constant. We assume that the storage unit has capacity $\overline{Q}_s$, and renewable curtailment is not allowed. Below, we show that, when the time horizon T is large, any affine policy would fail to support the above level of uncertainty. To see this, note that since $R_g = \pm 1/n$, any affine policy can assign at most $1/n$ fraction of the uncertainty to generator g at any time, without violating its ramp limit. On the other hand, any affine policy can assign at most $2\overline{Q}_s/T$ fraction of the uncertainty to the storage. (Otherwise, regardless of how the baseline $D^{\text{main}}(t)$ is chosen, the worst-case total energy dispatched to the storage will exceed $\overline{Q}_s$.) Thus, regardless of the storage size $\overline{Q}_s$, if $T > n\overline{Q}_s$, then any affine policy can support *at most* $3/n$ *fraction of the uncertainty* in total. In the above example, the curtailment may help to restore the system reliability only if we curtail a significant amount of renewable energy, unless the storage capacity $\overline{Q}_s$ increases proportionally with T. In contrast, based on our solution in the next section, we only need $\overline{Q}_s = \frac{1}{2}(n-1)$ to support the entire level of uncertainty above, even when $T \to \infty$. (See Theorem 7 and the discussion in Sec. III-C.) In summary, the difference in the supportable level of uncertainty between affine policies and our solution can be arbitrarily large as n increases. Please also see Sec. V-B for additional numerical results.

[2]Note that by definition, $F(\cdot,\cdot) \neq \emptyset$ at day-ahead RA also implies that $F(D(1{:}t), Q(t-1)) \neq \emptyset$ at all time t during real-time operations.

III. A Pair of Generator and Storage Unit

To develop our robust solution, we first study the interaction within a pair of components: a generator g and an energy storage unit s. In this section, we assume that the two components locate at the same bus. Thus, we omit the subscript b and denote the net-demand as $D(t)$. However, subscripts g and s are retained for clarity. Notice that, in this case, the safe-dispatch set consists of a set of 2-tuples $(P_g(t), Q_s(t))$. We note that in our previous work [14], we study a case of a fast generator paired with a slow generator. However, in [14] it is sufficient to record the output power of the slow generator in the safe-dispatch set, and thus the set becomes one dimensional. Unfortunately, the simple one dimensional set cannot serve the purposes in our case. Therefore, we must develop the characterization for the safe-dispatch set, despite the new difficulties involved with two dimensional space. In the remaining section, we fix t and $D(1{:}t)$.

A. Necessary Conditions for $F(D(1{:}t), Q_s(t-1)) \neq \emptyset$

Given the storage capacity $\overline{Q}_s$, we first derive necessary conditions for non-empty safe-dispatch set. Notice that, given $D(t)$ and $Q_s(t-1)$, because $P_g(t) + P_s(t) = D(t)$ must hold at time t, $P_g(t)$ uniquely determines $V(t) = (P_g(t), Q_s(t))$. Thus, for the purpose of characterizing $F(D(1{:}t), Q_s(t-1))$, we can focus on the conditions for $P_g(t)$ in terms of $Q_s(t-1)$. Suppose that the generator's output power at time t is $P_g(t)$. Due to the limited ramp rate R_g, at $t' \le t$, $P_g(t')$ can be bounded by $\underline{P}_g^e(t') \le P_g(t') \le \overline{P}_g^e(t')$, where

$$\overline{P}_g^e(t') = \min\{P_g(t) + (t'-t)R_g, P_g^{\max}\}, \quad (11)$$

$$\underline{P}_g^e(t') = \max\{P_g(t) - (t'-t)R_g, P_g^{\min}\}. \quad (12)$$

Further, to balance demand at t', we must have

$$\overline{P}_g^e(t') + P_s(t') \ge \max_{D(t'') \in \mathcal{D}_{t''}^{t'}} D(t'), \quad (13)$$

$$\underline{P}_g^e(t') + P_s(t') \le \min_{D(t'') \in \mathcal{D}_{t''}^{t'}} D(t'). \quad (14)$$

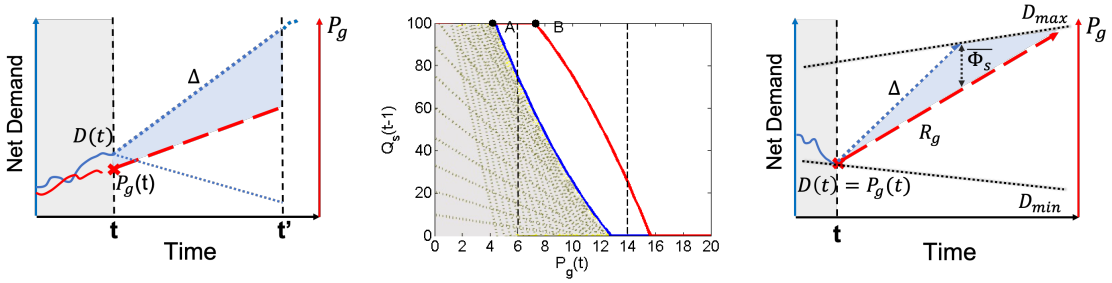

(a) (b) (c)

Fig. 1. (a) Given the generator's output $P_g(t)$, the least amount of required energy from the storage unit is represented by the blue area. (b) An outline of the safe-dispatch set under constraints (16) and (17). (Each dotted line corresponds to (16) for some t' t.) (c) An illustration of the storage size needed for meeting the fastest demand changes. Demand upper and lower bounds are of slopes and , respectively.

Notice that from (6), regardless of the sign of $_s(\ )$, we always have $Q_s(\ \ 1)\ \ Q_s(\ )\ \ \ _s(\ )$. Taking the telescopic sum of the upper bound of (13) for from t to t^0, since $\overline{P}^e_g(\ ) + Q_s(\ \ 1)\ \ Q_s(\ )\ \ \ \overline{P}^e_g(\ ) + \ _s(\ )$ $\max_{D(\ )2D^t} D(\ )$, we have

$$\sum_{=t}^{t^0} \overline{P}^e_g(\ ) + Q_s(t\ \ 1)\ \ Q_s(t^0) \quad \sum_{=t}^{t^0} \max_{D(\ )2D^t} D(\ ): \quad (15)$$

As $Q_s(t^0)\ 2\ [0; \overline{Q}_s]$, we must have, $8t^0 \quad t$,

$$Q_s(t\ \ 1) \quad \sum_{=t}^{t^0} \max_{D(\ )2D^t} D(\ )\ \ [P_g(t) + (\ \ t)R_g]\ : \quad (16)$$

This condition can be illustrated in Fig. 1a, where $D(t)$ increases with rate before reaching the net-demand upper bound $D^{\max}(t^0)$, and $P_g(t)$ tries to catch up the demand as fast as possible. In this case, the required storage level $Q_s(t\ \ 1)$ can be lowered bounded by the blue area between these two lines. Note that (16) for each t^0 is a linear constraint in terms of $(P_g(t); Q_s(t\ \ 1))$ (see dotted lines in shaded region in Fig. 1b). Thus, combining (16) for all t^0 leads to a convex constraint (see the lower blue solid curve in Fig. 1b). The blue solid curve represents the collection of system states where the storage unit has just enough energy to support the fastest increasing demand. Similarly, from (14) we must have:

$$Q_s(t\ \ 1) \quad \overline{Q}_s + \ _s \sum_{=t}^{t^0} \min_{D(\ )2D^t} D(\ )\ \ [P_g(t)\ \ (\ \ t)R_g]\ : \quad (17)$$

The upper red solid curve in Fig. 1b is obtained by taking intersection of (17) over all $t^0 \quad t$. We then combine (16) and (17) to produce a convex outer bound of the safe-dispatch set (see Fig.1b), which is termed *"leaf-region"* at time t given $D(t)$. Rearranging (16) and (17), we get: $8t_1; t_2 \quad t$,

$$^{\min}_{t_1}(D(1{:}t); Q_s(t\ \ 1)) \quad P_g(t) \quad ^{\max}_{t_2}(D(1{:}t); Q_s(t\ \ 1)); \quad (18)$$

where

$$^{\min}_{t_1}(D(1{:}t); Q_s(t\ \ 1)) \quad (19)$$
$$= \frac{1}{t_1\ \ t+1} \sum_{=t} [\max_{D(\ )2D^t} D(\ )\ \ (\ \ t)R_g]\ \ Q_s(t\ \ 1)\ ;$$

$$^{\max}_{t_2}(D(1{:}t); Q_s(t\ \ 1)) = \frac{1}{t_2\ \ t+1}\ \frac{1}{s}\ \overline{Q}_s\ \ Q_s(t\ \ 1)$$
$$+ \sum_{=t} \min_{D(\ )2D^t} D(\ ) + (\ \ t)R_g\ : \quad (20)$$

For example, points A and B in Fig. 1b correspond to $\max_{t_1\ t} {}^{\min}_{t_1}(D(1{:}t); \overline{Q}_s)$ and $\min_{t_2\ t} {}^{\max}_{t_2}(D(1{:}t); \overline{Q}_s)$, respectively. Thus, a necessary condition for $F(D(1{:}t); Q_s(t\ \ 1))$ is that

$$\max_{t_1\ t} {}^{\min}_{t_1}(D(1{:}t); Q(t\ \ 1)) \quad \min_{t_2\ t} {}^{\max}_{t_2}(D(1{:}t); Q(t\ \ 1)).$$

Similarly, the safe-dispatch set needs to be constrained by the storage's power limit $\overline{\ }_s$. Specifically, using $j\ \ (t^0)j \quad \overline{\ }_s$ in (13) and (14), we get, for all $t_1; t_2 \quad t$,

$$P_g(t) + (t_1\ \ t)R_g + \overline{\ }_s \quad \max_{D(t_1)2D^t_{t_1}} D(t_1); \quad (21)$$

$$P_g(t)\ \ (t_2\ \ t)R_g\ \ \overline{\ }_s \quad \min_{D(t_2)2D^t_{t_2}} D(t_2): \quad (22)$$

Thus, we have

$$\max_{t_1\ t} {}^{\min}_{t_1}(D(1{:}t))\ \ P_g(t)\ \ \min_{t_2\ t} {}^{\max}_{t_2}(D(1{:}t)); \quad (23)$$

where

$$^{\min}_{t_1}(D(1{:}t)) = \max_{D(t_1)2D^t_{t_1}} D(t_1)\ \ (t_1\ \ t)R_g\ \ \overline{\ }_s;$$
$$^{\max}_{t_2}(D(1{:}t)) = \min_{D(t_2)2D^t_{t_2}} D(t_2) + (t_2\ \ t)R_g + \overline{\ }_s.$$

A necessary condition for $F(D(1{:}t); Q_s(t\ \ 1))$ is then $\max_{t_1\ t} {}^{\min}_{t_1}(D(1{:}t)) \quad \min_{t_2\ t} {}^{\max}_{t_2}(D(1{:}t))$. Note that the safe-dispatch set is trimmed again by this condition (see the vertical dashed lines in Fig. 1b). Hence, the remaining part of the leaf-region between these two vertical dashed lines would be referred as the *"cropped leaf-region"* (CLR) at time t given $D(t)$.

Now, we can derive important necessary conditions on the required storage capacity for grid reliability. Here, we study a special uncertainty set with linear and symmetric net-demand upper and lower bounds. As shown in Fig.1c, $D^{\max}(\ )$ and $D^{\min}(\ )$ are straight lines with slope 0 and 0, respectively. For a long planning horizon, we present a lemma for the lower bound on the required storage capacity to achieve grid reliability as follows.

Lemma 4 (Minimum Storage Size)**.** *Suppose that the demand upper/lower bounds are linear and symmetric. For any* > 0, $9T_0$ *such that, for all* T $t+T_0$, *to ensure* $F(D(1{:}t); Q_s(t\ \ 1)) \neq$; *for some* $Q_s(t\ \ 1)$, *the storage size* $\overline{Q}_s$ *and power limit* $\overline{\ }_s$ *must satisfy*

$$\overline{Q}_s \quad \frac{\mathrm{Gap}(t)^2}{2}\ \frac{1}{R_g}\quad \frac{1}{\ } \quad ; \tag{24}$$

$$\overline{\ }_s \quad \mathrm{Gap}(t)\frac{R_g}{\ } \quad ; \tag{25}$$

respectively, where $\mathrm{Gap}(t) = D^{\max}(t) \quad D^{\min}(t)$.

Note that the small reduction in (24) and (25) reflects the fact that the storage requirement can be lower if the time horizon T is short (because the shaded triangle in Fig 1c is cut short). This will approach zero when the time horizon T is long. Also, notice that $\overline{Q}_s$ and $\overline{\ }_s$ are both inversely related to R_g. This is consistent with the intuition that a less flexible generator needs to pair with a more powerful storage unit to guarantee the robustness of the system.

We briefly sketch the idea of the proof. Suppose that the current net-demand is $D(t){=}D^{\min}(t)$. We can show that there must exist some $(P_g(t); Q_s(t)) \ 2\ F(D(1{:}t); Q_s(t\ \ 1))$ such that $P_g(t) \quad D^{\min}(t)$. Otherwise, we can show that, if $D(t^0){=}D^{\min}(t)$ for all $t^0\ \ t$, all decision points in future safe-dispatch set $F(D(1{:}t^0); Q_s(t^0\ \ 1))$ must also satisfy $P_g(t^0){>}D(t^0)$, which implies that the storage is always in charging state. However, this contradicts to $F(D(1{:}t); Q_s(t\ \ 1)) \neq$; since the storage's capacity limit would eventually be violated as T ! 1 and $P_g(t^0) > D(t^0)$. Now, suppose the future net-demand increases at the fastest rate until it reaches its upper bound (see Fig. 1c). Since $P_g(t^0) \quad D^{\min}(t^0)$, a lower bound for $\overline{Q}_s$ is given by the shaded blue area, i.e., the right-hand side of (24). Further, the length of the vertical line in Fig. 1c gives a lower bound of (25) for $\overline{\ }_s$. Note that these conditions are independent of $_s$. The reason is that when we perform a similar analysis for charging, it will always require a smaller storage size. (See details in technical report [18].)

B. Sufficient Conditions for $F(D(1{:}t); Q_s(t\ \ 1)) \neq$;

According to the analysis in Section III-A, for $F(D(1{:}t); Q_s(t\ \ 1)) \neq$; to hold, given $D(t)$, it is necessary that the CLR in Fig. 1b must be non-empty. In other words, there exists *some* $Q_s(t\ \ 1)\ 2\ [0; \overline{Q}_s]$ that intersects the CLR horizontally, i.e., $h(D(1{:}t); Q_s(t\ \ 1)) \neq$; for some $Q_s(t\ \ 1)$, where

$$\begin{array}{l} h(D(1{:}t); Q_s(t\ \ 1)) = \\ \quad \max\ \max\limits_{t_1\ \ t}\ \underline{\ }^{\min}_{t_1}(D(1{:}t); Q_s(t\ \ 1)); \max\limits_{t_1\ \ t}\ \underline{\ }^{\min}_{t_1}(D(1{:}t)) \ ; \\ \quad \min\ \min\limits_{t_2\ \ t}\ \underline{\ }^{\max}_{t_2}(D(1{:}t); Q_s(t\ \ 1)); \min\limits_{t_2\ \ t}\ \underline{\ }^{\max}_{t_2}(D(1{:}t)) \ : \end{array} \tag{26}$$

However, this condition does not imply that $F(D(1{:}t^0); Q_s(t^0\ \ 1)) \neq$; at a future time $t^0 > t$ because the value of $Q_s(t^0\ \ 1)$ cannot be arbitrarily chosen. In other words, it is possible that the cropped leaf region at t^0 does not intersect with $Q_s(t^0\ \ 1)$, which is determined by the decisions $Q(t_1); t_1 = t; : : : ; t^0\ \ 1$ (cf. (6) and (7)). Note that, in [14], we showed that similar conditions are both necessary and sufficient, thanks to the simplicity of one-dimensional safe-dispatch set. In sharp contrast, here the property no longer holds due to the complexity from two-dimensional set (26). In particular, the set (26) involves much more complex dependency between decision variables across stages. As a key contribution of this work, we introduce the following geometric property of the CLR (termed flat-top/flat-bottom property). The property effectively breaks the dependency across stages, and thus helps to develop simpler sufficient conditions of reliability.

Definition 5 (Flat-top/Flat-bottom)**.** A non-empty "CLR" given by conditions (16)-(17) and (21)-(22) is *"flat-top"* if the horizontal line $Q_s(t\ \ 1) = \overline{Q}_s$ intersects the "leaf-region", i.e., (26) holds with $Q_s(t\ \ 1) = \overline{Q}_s$. Similarly, it is *"flat-bottom"* if the horizontal line $Q_s(t\ \ 1) = 0$ intersects the "leaf-region", i.e., (26) holds with $Q_s(t\ \ 1) = 0$.

An example of a "flat-top" and "flat-bottom" CLR is shown in Fig. 1b. Thanks to the convexity of the "leaf-region", the "flat-top/flat-bottom" property implies that, for any $Q_s(t\ \ 1)\ 2\ [0; \overline{Q}_s]$, there must exists a non-empty set of decisions for $P_g(t)$. Thus, the above-mentioned difficulty due to the coupling between $Q_s(t\ \ 1)$ and $P_g(t\ \ 1)$ is avoided. The following theorem is the first main result of our work, which shows that this property is sufficient for reliability.

Theorem 6. *Given* $D(1{:}t)$, *if, for all* $t^0 \quad t$ *and every* $D(t^0)\ 2\ D^t_{t^0}$, *the "cropped leaf-regions" are both "flat-top" and "flat-bottom", there must exist a causal and robust real-time dispatch algorithm . Further, may choose any dispatch decision* $(P_g(t); Q_s(t))$ *from the following set*

$$\begin{array}{l} F^0 = \{(P_g(t); Q_s(t))\ P_g(t)\ 2\ h(D(1{:}t); Q_s(t\ \ 1)); \\ \qquad\qquad Q_s(t) = P_g(t) + Q_s(t\ \ 1) \quad D(t)\}; \end{array} \tag{27}$$

where $h(D(1{:}t); Q(t\ \ 1))$ *is the interval as described in* (26).

Sketch of Proof. The flat-top/flat-bottom property implies that the set $h(D(1{:}t); Q_s(t\ \ 1))$, and thus F^0s must be non-empty. Suppose that we choose $(P_g(t); Q_s(t))\ 2\ F^0$. The equality $Q_s(t) = P_g(t) + Q_s(t\ \ 1) \quad D(t)$ ensures that the net-demand $D(t)$ at time t can be balanced by $(P_g(t); Q_s(t))$. We next show the reliability for all future $t^0 > t$ by constructing a causal real-time dispatch algorithm that is robust given $D(1{:}t)$. Algorithm essentially picks a dispatch level from the interval $h(D(1 : t^0); Q_s(t^0\ \ 1))$, while satisfying the generator's ramping constraint from $P_g(t^0\ \ 1)$. See our technical report [18] for detailed proof for the sufficiency of the algorithm. □

Remark: We note that Theorem 6 is crucial for the rest of the analysis in this section because it successfully breaks the coupling between time t and $t\ \ 1$. Instead of keeping track of previous decisions to ensure $F(D(1{:}t); Q_s(t\ \ 1)) \neq$;, it is now sufficient to verify the CLR at time t, which tremendously simplifies the analysis. Note that only a minor loss of optimality occurs in such decoupling, since the derived sufficient conditions are tight in some cases.

Despite the significance of Theorem 6, checking the the flat-top/flat-bottom property for every value of $D(t')$ can still be tedious. To develop more efficient approaches, we again focus on the special case with linear and symmetric net-demand bounds (see Lemma 4 and Fig. 1c). The following theorem shows that the flat-top/flat-bottom property can indeed be verified in a simple way.

Theorem 7. *Given the uncertainty set D with symmetric bounds (parameterized by), the "cropped leaf-region" at time t for every $D(t)$ is "flat-top" and "flat-bottom" if the storage size $\overline{Q}_s$ and power limit $\overline{\ }_s$ satisfy the following:* $\overline{Q}_s \quad \frac{\mathrm{Gap}(t)^2}{2}\frac{1}{R_g} \quad \frac{1}{} \quad$ *and* $\overline{\ }_s \quad \mathrm{Gap}(t)\frac{R_g}{}$.

Proof. See Appendix A. □

Note that we do not mean to use the result of Theorem 7 to size generators or storage units in any long-term planning stage. Rather, the result becomes a building block later for the general multi-bus case, where demand will be split among virtual generator-storage pairs with varied capacity.

Next, we extend the result of Theorem 7 to the general cases with arbitrary upper and lower bounds. Note that the minimum requirement for $\overline{Q}_s$ and $\overline{\ }_s$ may not happen at the two extreme scenarios when the net-demand realization is equal to its upper/lower bound. Note that although Theorem 7 is based on the same for the upper and lower bounds of the uncertainty, we can apply the result to more general uncertainty sets by finding an outer approximation set with linear and symmetric bounds (parameterized by) that contains the original uncertainty set. Specifically, at time t, we find the value of as follows: consider a time-dependent (t) such that

$$(t) = \max\{\ ^u(t);\ ^l(t)\}; \tag{28}$$

where $^u(t) = \max\ \max_{t'>t}\frac{D^{\max}(t')\ D^{\max}(t)}{t'\ t};0$ and $^l(t) = \min\ \min_{t'>t}\frac{D^{\min}(t')\ D^{\min}(t)}{t'\ t};0$ *:* Plugging (t) and $\mathrm{Gap}(t)$ into (24) and (25), and taking a maximum over all time t, we obtain the following sufficient conditions for the storage size and power limit for the general case:

$$\overline{Q}_s = \max_t\left\{\frac{\mathrm{Gap}(t)^2}{2}\ \frac{1}{R_g\ (t)}\quad\frac{1}{(t)}\right\}; \tag{29}$$

$$\overline{\ }_s = \max_t\left\{\mathrm{Gap}(t)\frac{R_g}{(t)}\right\}: \tag{30}$$

C. Discussion & Comparison with Prior Work

From Theorem 7 and Lemma 4, it is not hard to find that our conditions for the safe-dispatch set are quite accurate. In fact, for the cases with constant net-demand bounds (i.e., =0) and very long planning horizons $T \to 1$, the conditions in Theorem 7 are both sufficient and necessary for $F(D(1{:}t);Q_s(t\ \ 1))$. To the best of our knowledge, for the first time in the literature, the required storage capacity for reliable grid operations under multistage uncertainty is precisely characterized. The intuitions are as follows. Suppose we take away the storage to leave the generator g only. Then, generator g's ramp speed must satisfy R_g . The extra storage s enables a generator with $R_g <$, at the "price" of meeting the minimum storage requirements specified in Theorem 7. More specifically, the required storage capacity $\overline{Q}_s$ increases with and decreases with R_g. If $\overline{\ }_s$ is large, as approaches infinity, the storage capacity $\overline{Q}_s$ approaches $\frac{\mathrm{Gap}(t)^2}{2(R_g\ )} < 1$. Therefore, these results illustrate novel insights for operating energy storage in future power grid under high renewable uncertainty.

Another highlight for the conditions in Theorem 7 is that they are independent of the time horizon T. Recall from the example in Section II-D, if we do not allow renewable curtailment, affine policies in [9] may require storage capacity to increase linearly in T. Our proposed conditions overcome the drawbacks in [9] because we successfully exploit the complementary capabilities of the generator and the storage, which leads to much more efficient storage utilization compared to [9]. We will verify these statements later in the simulation results in Section V.

IV. The Multi-bus Scenario

Next, we study the reliability assessment and real-time dispatch for general power systems with multiple buses. In this case, deriving the exact $F(D(1{:}t);Q_s(t\ \ 1))$ becomes intractable because of high dimensionality. However, we can still manage to obtain a subset of the exact $F(D(1{:}t);Q_s(t\ \ 1))$ for general power systems. The idea is similar to the *demand splitting* in [14], where a fraction of the total net-demand uncertainty was sent to each resource group (i.e., a pair of generator and storage in our case) based on pre-calculated *splitting factors*. Therefore, to fully exploit the benefit of generator-storage pairing, we implement the following: 1) Each storage unit is split into multiple *virtual storage units* (of potentially different sizes); 2) We form VGSPs by pairing the virtual storage units with generators; 3) Once the pairing is done, we can send the future net-demand uncertainty to every VGSP, and check the resource adequacy for each VGSP separately using our results developed in Sec. III.

We note that similar pairing ideas have been used in [14] to create virtual pairs of fast and slow generators. Compared to generator pairing, however, the setting of generator-storage pairing is significantly more challenging due to: (i) a new state-inconsistency issue when the storage has efficiency loss (Sec. IV-A) and (ii) the difficult in ensuring transmission limits when the storage and generator are on different buses (Sec. IV-C). Next, we first describe the elements of the VGSP idea, and then explain how we address these two challenges.

A. Creating VGSPs

For each physical generator g, we create N_s virtual generators, one for each storage unit $s; s = 1;\dots;N_s$. We index each of these virtual generators by $(g;s)$, with the corresponding maximum power $P^{\mathrm{vmax}}_{(g;s)}$, minimum power $P^{\mathrm{vmin}}_{(g;s)}$ and ramp limit $R^{\mathrm{v}}_{(g;s)}$. Similarly, each storage unit s is divided into N_g virtual storage units, with corresponding capacity limit $Q^{\mathrm{vmax}}_{(g;s)}$ and power limit $\overline{\ }^{\mathrm{v}}_{(g;s)}$, each of which is then paired with a virtual generator to form a VGSP $(g;s)$.

Next, we specify the conditions for such splitting to be feasible. Similar to [14], the total capability of the virtual generator or storage units must be consistent with the corresponding

physical units. However, here we face a new difficulty due to the use of storage. In contrast to the case $\eta = 1$ in [15], when $\eta < 1$, discrepancy may occur when combining the charging and discharging decisions across the virtual storage units into a single decision on the physical storage unit. To see this, suppose that a physical storage s is divided into two virtual units s_1 and s_2. Since each VGSP is first independently dispatched to meet a given fraction of the uncertain demand, it is possible that $P^{\rm v}_{s_1}(t) = -P^{\rm v}_{s_2}(t) > 0$, i.e., the dispatch decision is to charge virtual storage s_2 and discharge s_1 by the same amount. Obviously, to obtain a decision for dispatching the *physical* storage, the central controller (i.e., ISO) should combine these two opposite decisions, e.g., by dispatching the total power $P^{\rm v}_{s_1}(t) + P^{\rm v}_{s_2}(t) = 0$. Now, if we want to maintain the same physical storage state, then the physical storage should be discharged. However, this is then inconsistent with the dispatch power $P^{\rm v}_{s_1}(t) + P^{\rm v}_{s_2}(t) = 0$.

Below, we develop Lemma 8 to address the sub-optimality in terms of reliability. Note that in the above example, if we could use another generator to provide a negative power of $P^{\rm v}_{s_1}(t) \ge -P^{\rm v}_{s_2}(t)$, then both the storage state and the dispatch power can be viewed as consistent across physical and virtual storage. Therefore, our idea is to set aside some ramp-down capabilities of generators as reserves to provide such negative power. The following lemma gives an upper bound on the largest magnitude of the negative power that needs to be provided.

Lemma 8. *Suppose a physical storage unit s (parameterized by $[Q_s(t); \overline{Q}_s, \eta_s(t), \eta_s]$) is divided into K virtual units $\{[Q_i(t); \eta_i(t), \overline{Q}_i, \eta_i], i \in [1{:}K]\}$. To maintain both the dispatch power and the total energy level of all virtual storage units to be consistent with $Q_s(t)$, the amount of additional discharge of the physical storage, $O(t)$, satisfies*

$$0 \le O(t) \le (1/\eta_s - 1)\overline{Q}_s/2, \quad \text{at any time } t.$$

Note that this additional ramp resource to produce O is zero if $\eta_s = 1$, but is positive if $\eta_s < 1$.

Proof. See details in Appendix B. □

Using Lemma 8, we can now state the precise conditions for generator splitting (31)-(36) and storage splitting (37)-(38) to be feasible. Notice that a reserved amount of ramp-down rate $\sum_{s\in S}\overline{r}_{(g;s)}$ is taken from each generator g in (36) to compensate for the potential inconsistency discussed in Lemma 8. The parameters for virtual generators must satisfy the following.

$$\sum_{s\in S} P^{\rm vmax}_{(g;s)}(t^0) = P^{\rm max}_g, \forall g \in G, \forall t^0 \quad (31)$$

$$\sum_{s\in S}[P^{\rm vmin}_{(g;s)}(t^0) - r_{(g;s)}(t^0)] = P^{\rm min}_g, \forall g \in G, \forall t^0 \quad (32)$$

$$\sum_{s\in S}[R^{\rm v}_{(g;s)}(t^0) + \overline{r}_{(g;s)}(t^0)] = R_g, \forall g \in G, \forall t^0 \quad (33)$$

$$0 \le P^{\rm vmin}_{(g;s)}(t^0) \le P^{\rm vmax}_{(g;s)}(t^0), \ \forall (g;s) \in G \times S, \forall t^0 \quad (34)$$

$$R^{\rm v}_{(g;s)}(t^0) \ge 0, \ \overline{r}_{(g;s)}(t^0) \ge 0, \ \forall (g;s) \in G \times S, \forall t^0 \quad (35)$$

$$\sum_{g\in G}\overline{r}_{(g;s)}(t^0) \le (1/\eta_s - 1)\overline{Q}_s/2, \ \forall s \in S, \forall t^0 \quad (36)$$

$$\sum_{g\in G} Q^{\rm vmax}_{(g;s)}(t^0) = \overline{Q}_s, \quad \forall s \in S, \forall t^0 \quad (37)$$

$$\sum_{g\in G} \overline{\eta}^{\rm v}_{(g;s)}(t^0) = \overline{\eta}_s, \quad \forall s \in S, \forall t^0 \quad (38)$$

B. Demand Splitting for VGSPs

Next, we specify the demand splitting procedure to send fractions of the future uncertainty to the VGSPs. For the net-demand, we define its main part as $D^{\rm main}_b(t_0) = (\max\{D_b(t_0)\} + \min\{D_b(t_0)\})/2$. There is a decision $P^{\rm main}_{(g;s)}(t^0)$ for each VGSP $(g;s)$ that balances the sum of the main part of net-demand, i.e.,

$$\sum_{b\in B} D^{\rm main}_b(t^0) = \sum_{(g;s)\in G\times S} P^{\rm main}_{(g;s)}(t^0), \forall t^0 \quad (39)$$

Define the splitting factors $\alpha_{b;(g;s)}$ that satisfy

$$\sum_{(g;s)\in G\times S} \alpha_{b;(g;s)} = 1, \quad \forall b \in B \quad (40)$$

For the remaining uncertain demand $(D_b(t_0) - D^{\rm main}_b(t_0))$, we use affine splitting according to $\alpha_{b;(g;s)}$, such that

$$D^{\rm v}_{(g;s)}(t^0) = P^{\rm main}_{(g;s)}(t^0) + \sum_{b\in B} \alpha_{b;(g;s)}(D_b(t^0) - D^{\rm main}_b(t^0)), \quad \forall t^0 \le t; \forall (g;s) \in G \times S. \quad (41)$$

$D^{\rm v}_{(g;s)}(t^0)$ is then the total demand that is sent to VGSP $(g;s)$.

C. Transmission-line Limit Constraints

The above demand splitting onto VGSPs must satisfy the line limit constraints (8). In contrast to generator-only case in [14], here we face a new difficulty as the physical generator and the storage forming the same VGSP may locate at different buses. As a result, different ratios of power splitting between them will also change the power flows on transmission lines. However, when we form the VGSP, we do not know how power will be split between the virtual generator and virtual storage in the future. To address this difficulty, we introduce the following lemma such that, regardless of the power splittings between the virtual generator and storage within the same VGSP, at any time t the line-limit constraints will always hold.

Lemma 9. *For transmission line l, denote the power flow through l at time t as $f_l(t)$. Then, regardless of how power is split between the virtual generator and the virtual storage within the same VGSP, the transmission constraint $-f_l(t^0) \le TL_l$ holds if*

$$\sum_{b\in B} S_{l;b}\Big(D_b(t^0) - \sum_{(g;s):g\in G_b} D^{v}_{(g;s)}(t^0)\Big) + \gamma_{g;s}\Big| \le TL_l, \quad (42)$$

where $\gamma_{g;s} = \sum_{(g;s)} S_{l;B(g)} - S_{l;B(s)}\overline{\eta}^{\rm v}_{(g;s)}$; and $B(\cdot)$ returns the bus index where the generator or storage unit locates.

Proof. A sketch of the proof is available in Appendix C. □

In Lemma 9, the variable $\gamma_{g;s}$ corresponds to an upper bound on the maximum power change on line l due to the unknown power splitting between the virtual generator and virtual storage. Based on Lemma 9, we only need to ensure that the line limit is met for each possible value of $D_b(t^0) \in D^{t^0}_{[1:t]}$ and $D^{\rm v}_{(g;s)}(t^0)$ according to (41), $\forall t^0 \le t$.

D. Non-empty Safe Dispatch Set

So far we have specified the conditions to split uncertain demand onto VGSPs. In addition, we need to ensure that the parameters of VGSP $(g;s)$ and the uncertain net-demand $D^{\mathrm{v}}_{(g;s)}(t')$ in (41) produces a non-empty safe-dispatch set (recall from Sec. III-B):

$$\{P^{\mathrm{vmax}}_{(g;s)}, P^{\mathrm{vmin}}_{(g;s)}, R^{\mathrm{v}}_{(g;s)}, Q^{\mathrm{vmax}}_{(g;s)}, \underline{\ }^{\mathrm{v}}_{(g;s)}, P^{\mathrm{main}}_{(g;s)}(t'), \sim g \text{ satisfy (16)-(17),(21)-(22),(29)-(30)}, \quad \forall (g;s) \in G \times S \tag{43}$$

Let $Z(t) = \{P^{\mathrm{vmax}}_{(g;s)}, P^{\mathrm{vmin}}_{(g;s)}, R^{\mathrm{v}}_{(g;s)}, Q^{\mathrm{vmax}}_{(g;s)}, \underline{\ }^{\mathrm{v}}_{(g;s)}, Q^{v}_{(g;s)}(t-1), \alpha_{b;(g;s)}, P^{\mathrm{main}}_{g;s}(t'), P_g(t), \forall t' \le t, \forall g \in G, \forall s \in S, \forall b \in B\}$ denote the set of all decision variables at time t. Finally, the decision variables of the virtual generators and virtual storage units must be mapped back to the physical units to produce a safe dispatch decision $(\mathbf{P}(t), \mathbf{Q}(t))$ for time t according to the following.

$$P^{\mathrm{v}}_{(g;s)}(t), Q^{\mathrm{v}}_{(g;s)}(t) \in F^{Z(t)}_{(g;s)}\left(D(1{:}t), Q^{\mathrm{v}}_{(g;s)}(t-1)\right), \forall (g;s) \tag{44}$$

$$\sum_{g \in G_b} P_g(t) = \sum_{(g;s):g \in G_b} [P^{\mathrm{v}}_{(g;s)}(t) - r_{(g;s)}(t)], \quad \forall b \in B \tag{45}$$

$$\sum_{(g;s):g \in G} Q^{\mathrm{v}}_{g;s}(t') = Q_s(t'), \quad \forall t' = t-1, t, \forall s \in S \tag{46}$$

$$\sum_{b \in B} D_b(t) = \sum_{g \in G} P_g(t) + \sum_{s \in S} [Q_s(t-1) - Q_s(t)] \tag{47}$$

$$r_{(g;s)}(t) \le \overline{r}_{(g;s)}(t), \quad \forall (g;s) \in G \times S \tag{48}$$

$$\underline{\ }_s \le Q_s(t-1) - Q_s(t) \le \overline{\ }_s, \text{ if } t \ge 2, \forall s \in S \tag{49}$$

$$|P_g(t) - P_g(t-1)| \le R_g, \quad \text{only if } t \ge 2, \forall g \in G. \tag{50}$$

Remark. Note that the pre-computed splitting factors $\alpha_{b;(g;s)}$'s are only used to compute the decisions at time t. In the future, they can be recomputed to allow for correction when future uncertainty is revealed.

E. Real-time Dispatch and Reliability Assessment

As we mentioned before, RA and real-time dispatch problems are closely related. For ease of exposition, we first go straight to the real-time dispatch and formulate the following optimization problem.

$$\underset{Z(t)}{\text{minimize}} \quad Cost(\mathbf{P}(t)) \tag{51a}$$

$$\text{subject to} \quad \text{Constraints (31)-(50).} \tag{51b}$$

Note that the optimal solution $Z^*(t)$ of (51) determines the demand splitting among VGSPs and how physical generator/storage units are divided into virtual ones. While (51) focuses on real-time dispatch, similar expressions can be obtained for RA or for the safe-dispatch subset, i.e.,

$$F^{\mathrm{VGSP}}(D(1{:}t)) = \{[\mathbf{P}(t), \mathbf{Q}(t)] \mid \text{The parameter set } Z(t) \text{ exists such that (31)-(48) holds}\}. \tag{52}$$

The RA part can be similarly formulated as a minimization problem with any trivial objective function, subject to constraints (31)-(43) with the original uncertainty set D for entire T [14]. If a finite value is obtained from the minimization problem, then $F^{\mathrm{VGSP}}(D(1{:}t))$ must be non-empty for every t, i.e., the system passes the RA check.

V. Simulation Results

Next, we simulate our proposed multistage dispatch algorithm using MATLAB. Specifically, we cover two cases: 1) a generator-storage pair, and 2) a standard IEEE 30-bus power system [19] with a fleet of generators and storage. Since system reliability is our top concern, we compare our proposed algorithm with state-of-the-art robust affine policy [9].

A. A Generator + A Storage Unit on the Same Bus

First, we simulate a setting where a generator and an energy storage unit locate on same bus, in order to demonstrate that our proposed VGSP algorithm utilizes energy storage more efficiently compared to the affine policy in [9]. As mentioned earlier, curtailing renewable generation is both wasteful and costly, even though it may be used to improve the system reliability [9]. Thus, for the sake of algorithm comparison, renewable curtailment is not allowed in the simulation. Then, we evaluate the minimum required storage capacity for grid reliability under our proposed VGSP algorithm and compare with [9]. The data traces of load (Fig. 2a) and wind (Fig. 2b-2c) are obtained from Elia, the operator of transmission system in Belgium [16], with a scaling factor of 2. In practice, compared to renewable availability, load data is easier to predict at the ISO level. Hence, we adopt the common assumption in the literature that the load prediction is accurate at during the operation [9], i.e., the wind variability is the only source of net-demand uncertainty. We model the uncertainty set according to (1) and (2), and compute the related parameters using Elia's day-ahead prediction. In particular, we show the wind uncertainty bounds and variations in Fig. 2b and Fig. 2c, respectively. The generator can generate power (MW) in $[2000, 8000]$, with ramp rate 300MW/15min. Fig. 2d show the minimum required storage capacity to ensure grid reliability for different lengths of planning time. Clearly, the affine policy needs a significantly larger storage capacity as the operation horizon increases, while the required storage capacity for VGSP-RA only differs slightly. This observation aligns with our earlier discussion in Section III-C that sending a constant fraction of uncertainty to the storage can be inefficient. Instead, a better way to utilize storage is to pair it with generators.

B. IEEE 30-bus Test Case

Next, we test our algorithm on a standard IEEE 30-bus test case with 41 transmission lines [19]. We simulate our VGSP algorithm and state-of-the-art robust algorithm [9] based on AARO, and compare their performance. There are nineteen conventional generators, one wind farm (Bus 3), one pumped hydro energy storage unit (ES) with 90% charging efficiency, two loads (Bus 2 and 3) in the system. The conventional generators have 4 different types. The detailed specifications and location information of generators and ES are included in Table I. (See more details in [18].) We consider that ISO sends a dispatch decision every 15 min in real-time dispatching.

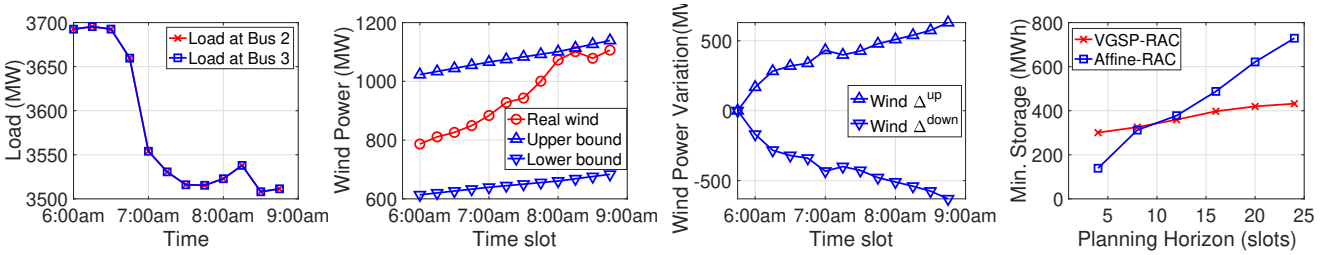

(a) Load profiles (b) Wind uncertainty bounds (c) Wind variations (d) Minimum storage size needed by VGSP-RA and affine policy [9].

Fig. 2. (a)-(c) experimental data for load and wind uncertainty; (d) Simulation results for Sec. V-A.

Table I. Types of Generators and Energy Storage

Type	Power Limit	Ramp Rate	Energy Price	Location
A	300-1100MW	20MW/15min	$40/MWh	1
B	210-300MW	10MW/15min	$32/MWh	2,13,22
C	190-450MW	30MW/15min	$60/MWh	13,22,23
D	0-100MW	60MW/15min	$100/MWh	1,2,22,23,27
	Capacity	Power Limit	Efficiency	Location
ES	750MWh	1000MW	90%	5

Table II. RA Decisions and Real-Time Generation Cost

Wind Scale	1	2	3	3.5	4
VGSP-RA	safe	safe	safe	safe	safe
Affine-RA	safe	safe	safe	safe	not safe
VGSP-ED($)	746,096	608,088	498,233	451,391	414,932
Affine-ED1($)	762,050	644,047	555,982	504,392	Inf
Savings	2.09%	5.58%	10.39%	10.51%	Inf
Affine-Curtail	767,802	662,426	587,876	549,724	509,903
Savings	2.83%	8.20%	15.25%	17.89%	18.63%

Again, we use Elia's load data and wind data in Fig. 2a-2c (over 3 hours, i.e, 12 slots). As shown in Fig. 2a, the loads at Bus 2 and Bus 3 are the same (total load about 7200MW). For renewable generation, the wind data for the same period of time is fed onto Bus 3. To admit some feasible solutions for both VGSP algorithm and affine policy [9] under the above data scale, we multiply transmission line limits from MATPOWER's IEEE 30-bus case file by 70 [20]. In Table II, we show the experimental results for RA and real-time dispatching under our proposed VGSP algorithm and the affine policy in [9]. We split into two cases depending on whether renewable curtailment is allowed. When the curtailment is prohibited, Row 2 and 3 in Table II show that, under the same set of resources, our proposed VGSP algorithm can guarantee grid safety up to a wind uncertainty scale of 4, while the affine policy fails beyond a wind scale of 3.5. This result justifies our discussion in Section III-C, thanks to the larger safe dispatch set by the VGSP algorithm over the affine policy. Next, we show that even at the wind scales lower than 3.5, such a higher level of safety assurance by VGSP algorithm can be translated to better economy gains. Indeed, Row 4-6 of Table II show that our proposed VGSP-ED algorithm always achieves lower fuel costs as compared to the affine policy with no wind curtailment (Affine-ED1). Further, we observe that the cost saving percentage increases from 2.09% to 10.51% as the wind uncertainty scale increases from 1 to 3.5. This is partly due to the fact that the day-ahead decisions can unnecessarily restrict the real-time dispatching in [9]. Specifically, the "policy-guided robust ED" decisions in [9] try to "follow" the worst-case trajectory identified by day-ahead RA, while VGSP algorithm does not have such restriction [14]. Finally, when renewable curtailment is allowed, [9] may safely operate at higher wind uncertainty level, but at the cost of significant renewable curtailment. To see this, we simulate the affine policy with possible wind curtailment (Affine-Curtail) in the last two rows in Table II. While Affine-Curtail can guarantee grid safety up to a wind scale of 4, its fuel costs are higher than both Affine-ED1 and VGSP-ED. This is because curtailment simply wastes "free" renewable energy. At a wind scale of 4, the saving of our VGSP-ED algorithm over Affine-Curtail is significant (18.63%).

C. Computational Complexity

Next, we show run-time results of our proposed solution. We run the simulations using MATLAB/CVX with Mosek solver on a MacBook with Intel Core i5 @ 2.3 GHz, 16GB Memory. To gain insight on the scalability of the proposed approach, we run our proposed VGSP-RA on an IEEE 118-bus test system with 54 generators. The running time for the 118-bus system is about 84s, while that for an 30-bus system with 19 generators is 18s (see further results in our technical report [18]).

VI. Conclusion

This work studies robust multistage decisions for operating both generators and energy storage to ensure grid reliability under significant renewable uncertainty. Following a divide-and-conquer paradigm, we first focus on a pair of generator and storage, and derive a very accurate characterization for the safe-dispatch set under multistage uncertainty. Then, by combining the ideas of VGSP pairing and demand splitting, we utilize the above results to develop an efficient robust algorithm for general multi-bus systems. The numerical results show that our proposed solution outperforms state-of-the-art affine policy in [9] in terms of reliability and economy. For future work, we will extend the approach to incorporate unit commitment and possible renewable curtailment.

References

[1] T. Mai, D. Sandor, R. Wiser, and T. Schneider, "Renewable Electricity Futures Study: Executive Summary," National Renewable Energy Laboratory, Golden, CO, Tech. Rep., 2012.

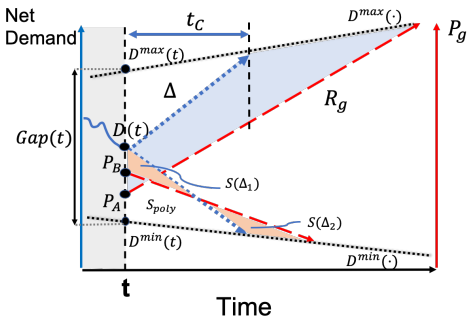

Fig. 3. The movement of A and B according to net-demand increase .

[2] J. Eyer, G. Corey, and S. N. Laboratories, *Energy Storage for the Electricity Grid: Benefits and Market Potential Assessment Guide*, ser. SAND (Series). Sandia National Laboratories, 2010.
[3] Federal Energy Regulatory Commission, "Order No.888," 1996.
[4] MISO Energy. [Online]. Available: https://www.misoenergy.org
[5] "Maintaining bulk power system reliability while integrating variable energy resources," NERC and CAISO, Tech. Rep., 2013.
[6] D. Bertsimas, E. Litvinov, X. A. Sun, J. Zhao, and T. Zheng, "Adaptive robust optimization for the security constrained unit commitment problem," *IEEE Trans. on Power Systems*, vol. 28, no. 1, February 2013.
[7] R. Jiang, J. Wang, and Y. Guan, "Robust unit commitment with wind power and pumped storage hydro," *IEEE Transactions on Power Systems*, vol. 27, no. 2, pp. 800–810, 5 2012.
[8] A. Lorca, X. A. Sun, E. Litvinov, and T. Zheng, "Multistage adaptive robust optimization for the unit commitment problem," *Operations Research*, vol. 64, no. 1, pp. 32–51, 2016.
[9] A. Lorca and X. A. Sun, "Multistage robust unit commitment with dynamic uncertainty sets and energy storage," *IEEE Transactions on Power Systems*, vol. 32, no. 3, pp. 1678–1688, May 2017.
[10] J. B. Rawlings and D. Q. Mayne, *Model predictive control: Theory and design*. Nob Hill Pub., 2009.
[11] M. Shahidehpour, C. Liu, H. Zhang, Q. Zhou, and T. Ding, "A two-layer model for microgrid real-time scheduling using approximate future cost function," *IEEE Trans. Power Systems*, 2021.
[12] A. Ben-Tal, S. Boyd, and A. Nemirovski, "Extending scope of robust optimization: Comprehensive robust counterparts of uncertain problems," *Mathematical Programming*, vol. 107, no. 1, pp. 63–89, 2006.
[13] D. Bertsimas, D. B. Brown, and C. Caramanis, "Theory and applications of robust optimization," *SIAM Rev.*, vol. 53, pp. 464–501, August 2011.
[14] S. Zhao, Y. Zou, X. Lin, D. Aliprantis, H. N. V. Pico, M. Chen, and A. Castillo, "Leveraging generators with complementary capabilities for robust multistage power grid operations," *IEEE Transactions on Control of Network Systems*, vol. 7, no. 3, pp. 1441–1452, 2020.
[15] Y. Zou, X. Lin, D. Aliprantis, and M. Chen, "Robust multi-stage power grid operations with energy storage," in *IEEE INFOCOM 2018*, Honolulu, HI, April 2018, pp. 2483–2491.
[16] Elia. Grid data. [Online]. Available: http://www.elia.be/en/grid-data
[17] A. Wood, B. Wollenberg, and G. Sheble, *Power Generation, Operation, and Control*. Wiley, 2013.
[18] Y. Zou, X. Lin, D. Aliprantis, and M. Chen, "Robust multi-stage power grid operations with energy storage," Purdue University, https://engineering.purdue.edu/%7elinx/papers.html, Tech. Rep., 2017.
[19] U. Washington, "Power systems test case archive." [Online]. Available: http://www2.ee.washington.edu/research/pstca/
[20] "Matpower." [Online]. Available: www.pserc.cornell.edu/matpower/

APPENDIX A
PROOF OF THEOREM 7

We can prove the theorem in the following two steps: 1) The uncropped "leaf-regions" given by (19) and (20) (i.e., without the power limits) for every $D(t)$ is both flat-top and flat-bottom; 2) The "cropped leaf-region" induced by power limits (21) and (22) will retain the flat-top/flat-bottom property. Due to space limit, we only show Step 1, which is precisely the result of Lemma 10 below. Step 2 can be shown similarly.

Lemma 10. *Given the uncertainty set D with symmetric bounds (parameterized by), the uncropped "leaf-region" for every $D(t)$ (without considering power limits) is "flat-top" and "flat-bottom" if the storage size satisfies*

$$\overline{Q}_s \quad \frac{\mathrm{Gap}(t)^2}{2} \quad \frac{1}{R_g} \quad \frac{1}{} : \tag{53}$$

.

Proof. We mainly focus on the proof of the "flat-top" part, as the proof of the "flat-bottom" part is similar. As shown in Fig. 3, suppose that the bounds of net-demand $D^{\max}(\,)$ and $D^{\min}(\,)$ are changing at rate and , respectively. Suppose that the net-demand is $D(t)$ at time t. Point P_A in Fig. 3 corresponds to the generator's lowest power that satisfies (16) with $Q_s(t \;\; 1) = \overline{Q}_s$, i.e., the shaded area between blue upward dotted line and red upward dash line is $\overline{Q}_s$. Similarly, Point P_B is the generator's highest power that satisfies (17) with $Q_s(t \;\; 1) = \overline{Q}_s$. The flat-top property in Fig. 1b thus corresponds to $P_B \quad P_A$. In order to prove that $P_B \quad P_A$ for all $D(t)$, we break into the following two steps: (i) Prove $P_B \quad P_A$ for $D(t) = D^{\min}(t)$; (ii) Noting that both P_A and P_B increase with $D(t)$, prove that $\frac{@P_B}{@D(t)} \quad \frac{@P_A}{@D(t)}$. We first show Step (i). If $D(t) = D^{\min}(t)$, then $P_B = D(t)$ since the orange triangles are simply empty. If $P_A \quad D(t) = D^{\min}(t) = P_B$, the area of the blue region would be at most $\frac{\mathrm{Gap}(t)^2}{2(R_g \quad)} \quad \frac{\mathrm{Gap}(t)^2}{2(\quad)}$: By (53), this area cannot be equal to $\overline{Q}_s$. Thus, P_A must be the same as or below P_B, i.e., $P_B \quad P_A$.

The next proof of (ii) is the key component of the lemma. Suppose that $D(t) = D \;\; 2 \; [D^{\min}(t); D^{\max}(t)]$. We first look at the rate of change $\frac{dP_A}{dD}$. In Fig. 3, P_A corresponds to the area of blue shaded region being equal to $\overline{Q}_s$, i.e.

$$\frac{1}{2}\frac{(D^{\max} \quad P_A)^2}{R_g} = \frac{1}{2}\frac{(D^{\max} \quad D)^2}{} + \overline{Q}_s: \tag{54}$$

This equation defines an implicit function between P_A and D. To get the rate of change on P_A w.r.t. D, we can differentiate both sides of (54)

$$\frac{dP_A}{dD} = \frac{D^{\max} \quad D}{D^{\max} \quad P_A}\frac{R_g}{} \quad \frac{R_g}{}; \tag{55}$$

where the last inequality comes from the fact that $P_A \quad D$, and thus $\frac{D^{\max} \quad D}{D^{\max} \quad P_A} \quad 1$. Next, we derive the derivative of P_B in similar way. As shown in Fig. 3, the interpretation of P_B is the generator's highest power such that the storage does not require any charging room for the future decreasing demand. That is to say, assuming $_s \quad 1$, the area $S(\;\; _2)$ of the triangle on the bottom-right (i.e., charging part) must be equal to $1= _s$ times the area $S(\;\; _1)$ of the triangle on the left (i.e., discharging part), i.e., $S(\;\; _1) = \; _s S(\;\; _2)$: We can add to both sides $_s$ times the area of the polygon S_{poly} in Fig. 3. Noting that $S(\;\; _1) = \frac{1}{2}\frac{(D \quad P_B)^2}{R_g}$, $S(\;\; _1)+S_{\text{poly}} = \frac{1}{2}\frac{(D \quad D^{\min})^2}{}$ and $S(\;\; _2)+S_{\text{poly}} = \frac{1}{2}\frac{(P_B \quad D^{\min})^2}{R_g}$, Eq. $S(\;\; _1) = \; _s S(\;\; _2)$ is equivalent to

$$(1 \quad _s)\frac{1}{2}\frac{(D \quad P_B)^2}{R_g} + \; _s\frac{1}{2}\frac{(D \quad D^{\min})^2}{} = \; _s\frac{1}{2}\frac{(P_B \quad D^{\min})^2}{R_g}: \tag{56}$$